

Pseudomonas aeruginosa alkaline protease exhibits a high renaturation capability

Mariola Andrejko¹✉, Anna Siemińska-Kuczer¹, Monika Janczarek², Ewa Janik³, Mirosława Bednarczyk³, Mariusz Gagoś³ and Małgorzata Cytryńska¹

¹Department of Immunobiology, ²Department of Genetics and Microbiology, ³Department of Cell Biology, Faculty of Biology and Biotechnology, Maria Curie-Skłodowska University, Lublin, Poland

Thermally induced unfolding and renaturation capability of alkaline proteases (AP) of three *Pseudomonas aeruginosa* strains, i.e. ATCC 27853 and two clinical isolates, were examined. Sequence analyses demonstrated a high level of *aprA* genes identity (99.24–99.8%) in these bacterial strains. The proteases retained 45–60% and 15% of their activity after pre-treatment at 60°C and 80°C, respectively, whereas pre-incubation at 90–95°C resulted in a higher level of activity than at 80°C. Zymography analyses and immunoblotting with AP antiserum suggested a high thermostability and renaturation capability of the studied enzymes in comparison to another *P. aeruginosa* protease, elastase B. An intrinsic capability of renaturation of *P. aeruginosa* AP was confirmed by fluorescence spectra of the native, thermally denatured, and renatured enzyme. The value of the fluorescence intensity of the denatured and subsequently cooled enzyme recovered to about 80% of the value of the native protein fluorescence intensity. Moreover, pre-incubation of the enzyme at 60°C and 90°C exerted only a slight effect on the intensity of absorbance and the shape of the amide I band, as demonstrated by Fourier transform infrared (FTIR) spectroscopy performed after subsequent cooling of the pre-treated enzyme. The results indicated a high renaturation capability of the *P. aeruginosa* AP proteins.

Key words: *Pseudomonas aeruginosa*, alkaline protease, zymography, renaturation, steady-state fluorescence spectroscopy, Fourier transform infrared spectroscopy

Received: 19 November, 2018; **revised:** 22 January, 2019; **accepted:** 20 February, 2019; **available on-line:** 04 March, 2019

✉e-mail: mariola.andrejko@poczta.umcs.lublin.pl

Abbreviations: AP, alkaline protease; BCIP, 5-bromo-4-chloro-3-indolyl-phosphate; DEAE-cellulose, diethylaminoethyl-cellulose; FTIR, Fourier transform infrared; NBT, nitro blue tetrazolium; PCR, polymerase chain reaction; PVDF, polyvinylidene difluoride; SDS-PAGE, sodium dodecyl sulfate polyacrylamide gel electrophoresis; IEF/SDS-PAGE, two-dimensional gel electrophoresis

INTRODUCTION

The *Pseudomonas aeruginosa* alkaline protease (EC 3.4.24.40) named aeruginolysin is a zinc-dependent metalloprotease. It is a member of the serralsin family and belongs to the metzincin superfamily of metalloendopeptidases (Rawlings *et al.*, 2010). Aeruginolysin is homologous to 50-kDa metalloproteinases secreted by *Serratia marcescens* and *Dickeya dadantii*. An analysis of *P. aeruginosa* aeruginolysin, *S. marcescens* metalloprotease, and protease C (PrtC), i.e. one of the four serralsins secreted by *D. dadantii*, had shown that these proteins

consist of an N-terminal catalytic domain of about 230 amino acid residues and a C-terminal calcium binding domain of approximately 240 amino acid residues (Okuda *et al.*, 1990; Guzzo *et al.*, 1991; Miyatake *et al.*, 1995). The catalytic domain contains an extended zinc-binding motif HEXXXHXUGUXH (X and U indicate an arbitrary and a bulky hydrophobic amino acid, respectively) and a conserved methionine located in a turn near the base of the metal binding pocket. The structural domain that folds into a β -roll stabilized with calcium ions contains a repetitive glycine-rich nanopeptide, characteristic for repeat-in-toxin (RTX) proteins, and a secretion signal located within the last 70 residues (Baumann *et al.*, 1993; Feltzer *et al.*, 2000; Zhang *et al.*, 2012). The genetic region for the synthesis and secretion of *P. aeruginosa* alkaline protease (AP) contains five open reading frames: *aprA* which is a structural gene of the protease, *aprI* which encodes a protease inhibitor, and *aprD*, *aprE*, and *aprF* genes, whose protein products are involved in secretion of the protease and constitute the Type 1 secretion system (T1SS) in *P. aeruginosa* (Duong *et al.*, 1992; Duong *et al.*, 1996; Hoge *et al.*, 2010).

Being one of the *P. aeruginosa* virulence factors, alkaline protease is produced during keratitis, otitis media, cystic fibrosis, and bacteraemia (Caballero *et al.*, 2001; Leidal *et al.*, 2003; Guyot *et al.*, 2010; Butterworth *et al.*, 2012) and it is implicated in hydrolysis of many biologically important proteins, including cytokines (Parmely *et al.*, 1990), complement factors (Hong & Ghebrehiwet, 1992), matrix metalloproteinases (Twining *et al.*, 1993), γ -interferon and tumor necrosis factor- α (Horvat & Parmely, 1988; Parmely *et al.*, 1990).

Our previous report demonstrated that three *P. aeruginosa* strains, i.e. a reference strain ATCC 27853 and two human clinical isolates PA C124/9 and PA 02/18, displayed different profiles of secreted proteases depending on the strain and on the medium used for bacterial culture. We had confirmed presence of the *lasB* gene encoding elastase B and the *aprA* gene coding for alkaline protease in the genomes of the three *P. aeruginosa* strains analysed. Interestingly, the AP was produced mainly during bacterial growth in minimal M9 medium (Andrejko *et al.*, 2013). Our preliminary experiments revealed a surprising renaturation capability of the AP secreted by *P. aeruginosa* ATCC 27853. Although *P. aeruginosa* alkaline protease has been described (Okuda *et al.*, 1990; Guzzo *et al.*, 1991; Baumann *et al.*, 1993; Miyatake *et al.*, 1995; Bayoudh *et al.*, 2000; Rahman *et al.*, 2006; Patil & Chaudhari, 2009; Hoge *et al.*, 2010), such a capability has not been reported. To elucidate this issue further and to test if such a feature is characteristic for AP produced by this particular ATCC 27853 strain or whether it is shared

by alkaline proteases of other *P. aeruginosa* strains, in this paper we studied the thermally induced unfolding and renaturation capability of alkaline proteases of the three *P. aeruginosa* strains, in parallel with comparative sequence analysis of the *aprA* genes and AP proteins of these bacteria. Given that alkaline protease is considered as one of *P. aeruginosa* virulence factors implicated in many diseases, our results on AP unfolding and renaturation provide an additional insight into *P. aeruginosa* pathogenicity.

MATERIALS AND METHODS

Bacterial strains and culture conditions. A pyocyanin-producing *Pseudomonas aeruginosa* strain ATCC 27853 (ATCC) and two human clinical strains PA C124/9 (PA9) and PA 02/18 (PA18) were used in the study. The bacteria were grown overnight at 37°C in M9 minimal medium supplemented with monosodium glutamate (0.13 M), glycerol (0.1 M), and CaCl₂ (0.01 M) on a rotary shaker (120 rpm). For some experiments, the bacteria were cultured in Lysogeny Broth (LB medium, Sigma-Aldrich) as described in our previous report (Andrejko *et al.*, 2013).

DNA methods and sequence analysis. Standard techniques were used for genomic DNA isolation, agarose gel electrophoresis, PCR, and sequencing (Sambrook *et al.*, 1989). PCR amplifications of 1.5-kb long fragments containing the whole alkaline protease gene from *P. aeruginosa* PA C124/9, PA 02/18, and ATCC 27853 strains were performed using primers *aprA*-F (forward, 5'-CCTGATCKGGCCGATAACTGCAAT-3') and *aprA*-R (reverse, 5'-GGAAGACASCTATCAATTC-GAACAG-3'), and reaction conditions described earlier (Andrejko *et al.*, 2013). The PCR products obtained were purified on columns (A&A Biotechnology) and then sequenced using a BigDye terminator cycle sequencing kit (Applied Biosystems) and an ABI Prism 310 sequencer. The sequences generated in this study for the *aprA* gene of the *P. aeruginosa* PA C124/9, PA 02/18, and ATCC 27853 strains were deposited in NCBI GenBank under accession numbers: JX853448, JX853449, and JX853450, respectively. An analysis of the sequences at both, the nucleotide and amino acid level, was carried out using the FASTA and BLAST programs available at the European Bioinformatics Institute (Hinxton, UK) and the National Centre for Biotechnology Information (Bethesda, MD, USA). Alignment of the amino acid sequences of AP proteins of the *P. aeruginosa* strains and homologous proteases was done by using the Clustal Omega program (<http://www.ebi.ac.uk/Tools/services/>) (Sievers *et al.*, 2011).

Alkaline protease purification. Bacteria were cultivated in M9 medium under aerobic conditions at 37°C for 24 h with rotational shaking (120 rpm). Then, the bacterial cultures were centrifuged at 8000 × *g* for 20 min at 4°C to pellet the cells. The post-culture fluids were filtered through a 0.3 µm-pore-size filter (Millipore) to remove any remaining bacteria. Proteins secreted into the growth medium were precipitated from the filtrates with ammonium sulphate (90% saturation) at 4°C overnight. The precipitates were collected by centrifugation at 8000 × *g* for 20 min at 4°C, dissolved in 20 mM Tris-HCl pH 8.0, and dialysed overnight against the same buffer. The dialysed solutions were fractionated using anion-exchange chromatography on a DEAE-cellulose column (DE 52, Whatman) equilibrated with 20 mM Tris-HCl pH 8.0. Proteins bound to the column were eluted with a linear gradient of 0–0.7 M NaCl in the

same buffer. Fractions with proteolytic activity, eluted at 0.15–0.22 M NaCl, were pooled, concentrated with polyethylene glycol 20000 (PEG 20000), dialysed overnight against 20 mM Tris-HCl pH 8.0, lyophilized, and the final preparations were stored at –20°C. The protein concentration was estimated using the Bradford method and bovine serum albumin (BSA) as a standard (Bradford, 1976).

Proteolytic activity assay. The alkaline protease activity was measured using a modified method described by Howe and Iglewski (Howe & Iglewski, 1984). Samples containing 5 mg of the Hide powder azure (HPA, Sigma-Aldrich) dissolved in a buffer (0.4 ml) consisting of 20 mM Tris-HCl pH 8.0, and 1 mM CaCl₂, were mixed with 0.1 ml of the enzyme fraction. The reaction mixtures were incubated at 37°C for 60 min with constant rotation. An undissolved substrate was removed by centrifugation at 4000 × *g* for 5 min and the absorbance of the supernatants was determined at 595 nm.

Effect of temperature pre-treatment on alkaline protease activity. The enzyme solutions were pre-incubated for 30 min at different temperatures in a range of 40–95°C. To avoid a potential calcium-induced folding and stabilization of the AP proteins, the pre-treatment was carried out in the absence of Ca²⁺ ions (Zhang *et al.*, 2012). After rapid cooling of the samples in an ice bath, the enzymatic activity was measured under standard assay conditions described above. The relative activities were expressed as a percentage (%) of the maximum activity determined for each alkaline protease pre-incubated at 40°C.

Steady-state fluorescence spectroscopy. Fluorescence emission spectra were measured using an F-7000 spectrofluorometer (Hitachi) at 23°C. The excitation wavelength was set at 280 nm. The excitation and emission slits were 5 nm. The spectra were measured in samples with the same protein concentration. The protein samples were heated for 30 min at 60°C or 90°C. Next, the samples were cooled for 30 min at 4°C. The spectra were analyzed using Grams/AI 9.1 software.

Fourier transform infrared spectroscopy. All measurements were carried out on a Bruker Vertex 70 spectrometer equipped with a liquid N₂-refrigerated MCT detector. All spectra were recorded by attenuated total reflection (ATR) at room temperature (22°C). 20-µl samples with native protein or samples heated at 60°C and 90°C for 30 min and then cooled for 30 min at 4°C were deposited on the 20-reflection ZnSe crystal at the angle of incidence of 45°. The samples were quickly evaporated in an N₂ flux to obtain a homogenous film. The spectrometer was flushed with dry nitrogen gas for at least 30 min before the spectra were recorded. The FTIR measurements were recorded between 4000 and 800 cm⁻¹. Each spectrum was obtained by averaging 32 scans recorded at a resolution of 2 cm⁻¹. Prior to data analysis, the spectra were baseline-corrected and normalised using the vector normalisation method. The ATR-FTIR spectra were cut to include an amide I band (wavelengths between 1600 and 1700 cm⁻¹). The procedure was performed using the OPUS version 7.5 software. OPUS software was used to convert the FTIR absorbance spectra into second derivatives.

Polyacrylamide gel electrophoresis. Protein samples were separated by SDS-PAGE in 10% polyacrylamide gels under reducing or non-reducing conditions according to Laemmli (Laemmli, 1970). In some experiments, native-PAGE was used. For this purpose, polyacrylamide gels and an electrode buffer did not contain SDS, while the samples were prepared by addition of saccha-

rose and bromophenol blue to the final concentrations of 20% and 0.05%, respectively. Two-dimensional gel electrophoresis (IEF/SDS-PAGE) of the proteins was performed using a Protean System (BioRad) according to the manufacturer's instructions. ReadyStrip™ IPG Strips pH 3-10 were used for the first dimension (Andrejko & Mizerska-Dudka, 2012).

Zymography analysis. Gelatine zymography was conducted following the procedures described by Caballero and others (Caballero *et al.*, 2001). Samples of enzyme solutions (1 µg protein), non-treated or pre-treated at different temperatures, were electrophoresed under non-reducing conditions using 10% polyacrylamide gels with 0.1% gelatine at 4°C. The purified enzymes were also analysed by zymography after IEF/SDS-PAGE. In this case, the gels used for separation in the second dimension contained 0.1% gelatine. After electrophoresis, the gels were soaked twice for 30 min in 2.5% Triton X-100 for SDS removal and incubated at 37°C for 24 h in a gelatine gel substrate buffer (50 mM Tris-HCl pH 8.0, 10 mM CaCl₂, 1 µM ZnCl₂, 150 mM NaCl). The gels were stained for 60 min in 0.2% amido black and then destained in 10% acetic acid.

Immunoblotting. After electrophoretic separation (SDS-PAGE, native-PAGE, or IEF/SDS-PAGE), the proteins were electrotransferred onto PVDF membranes (Millipore) for 90 min at 350 mA. The membranes were blocked with 5% non-fat milk in Tris-buffered saline (TBS; 10 mM Tris-HCl pH 7.5, 0.9% NaCl). For identification of the alkaline protease, the membranes were probed with a polyclonal rabbit AP antiserum (1:1000) (kindly provided by Dr. R. Voulhoux). Alkaline phosphatase-conjugated goat anti-rabbit IgGs (1:30000) (Sigma-Aldrich) were used as secondary antibodies and immunoreactive bands were visualized by incubation with *p*-nitro blue tetrazolium chloride (NBT) and 5-bromo-4-chloro-3-indolyl phosphate (BCIP) (Blake *et al.*, 1984).

RESULTS

Purification and identification of alkaline proteases secreted by the *P. aeruginosa* strains

The alkaline proteases (AP) of the three *P. aeruginosa* strains were purified from the 24-h post-culture fluids by ammonium sulphate precipitation and ion-exchange chromatography on DEAE-cellulose. The results of zymography performed under non-reducing SDS-PAGE conditions revealed the presence of one 52 kDa band of proteolytic activity irrespective of the strain (Fig. 1A). Immunoblotting with the polyclonal rabbit AP antiserum clearly confirmed that the alkaline protease was responsible for the proteolytic activity detected in all of the final preparations (Fig. 1B). In addition, a single spot of proteolytic activity was detected when AP protein produced by the PA18 strain was analyzed by zymography after IEF/SDS-PAGE (Fig. 1C). It clearly corresponded to that of approx. pI 4.5 recognized by the anti-alkaline protease antibodies (Fig. 1D). The theoretical isoelectric point of this protein was calculated as pI 4.28 on the basis of amino acid sequence presented in Fig. 7.

Effect of temperature pre-treatment on the activity of alkaline proteases

The activity of the studied enzymes was measured after 30-min pre-incubation at different temperatures ranging from 40°C to 95°C and subsequent cooling at the ice

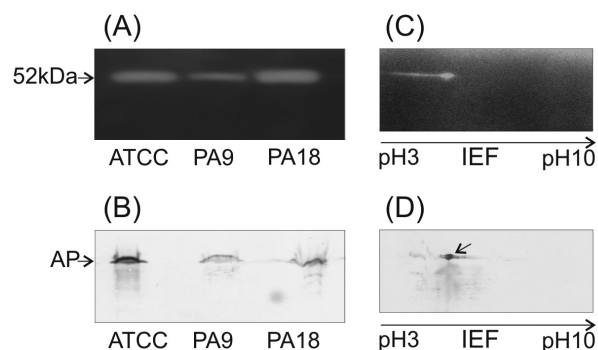


Figure 1. Identification of alkaline proteases of three *P. aeruginosa* strains in the final preparations obtained by ion-exchange chromatography on DEAE-cellulose.

(A, C) Alkaline protease zymography analysis and (B, D) detection by specific antibodies. The proteins (1 µg) were resolved by non-reducing SDS-PAGE in gelatine gels (A) and in standard gels (B) for zymography and alkaline protease detection, respectively. For the 2D electrophoresis (C, D), the alkaline protease produced by *P. aeruginosa* PA18 (2 µg of protein) was resolved in the first dimension by IEF pH 3–10. In the second dimension, the protein was separated by SDS-PAGE under non-reducing conditions in a gel containing 0.1% gelatine (C) and by standard SDS-PAGE (D) for zymography and alkaline protease detection, respectively. The gelatine gels were washed and stained as described in Materials and Methods. Alkaline protease was detected after transferring proteins onto PVDF membranes and probing with anti-*P. aeruginosa* alkaline protease antibodies (B and D). The results shown in (A, B) and (C, D) are typical representatives of at least five and three independent experiments, respectively. The positions of alkaline protease (AP) are marked by arrows. ATCC – reference strain, PA9 and PA18 – clinical isolates.

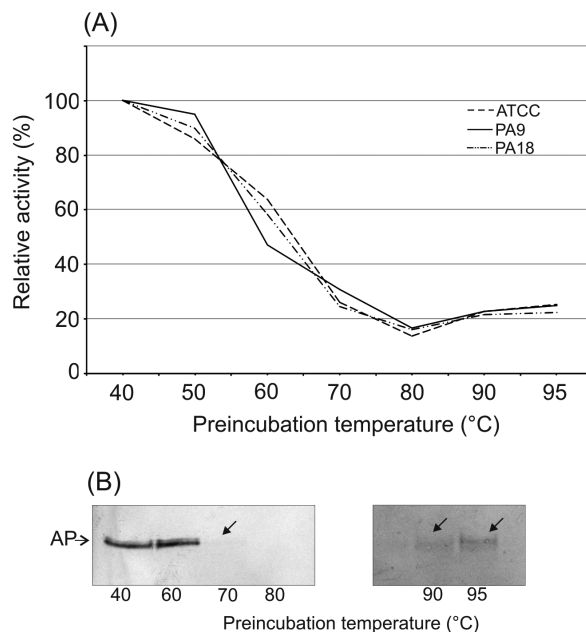


Figure 2. Effect of temperature on the activity of alkaline proteases.

The enzymes were pre-incubated at different temperatures in the range of 40–95°C for 30 min. (A) The remaining activity was determined with the Hide powder azure as a substrate under standard assay conditions (see Materials and Methods). The activity was expressed as a percentage of the value at 40°C, which was taken as 100%. (B) For alkaline protease detection, the samples (1 µg of protein) were resolved by native PAGE, transferred onto PVDF membranes, and probed with anti-*P. aeruginosa* alkaline protease antibodies. The immunoblottings shown are typical representatives of at least three independent experiments. ATCC – reference strain, PA9 and PA18 – clinical isolates.

Table 1. Effect of temperature on the activity of alkaline proteases

Temperature [°C]	ATCC [%]	PA9 [%]	PA18 [%]
50	90.27±3.69	90.17±3.92	90.40±3.65
60	56.37±6.99	56.20±7.01	56.07±6.62
70	27.10±2.69	26.57±2.31	15.43±1.25
80	15.43±1.25	15.33±1.30	15.03±1.24
90	23.13±0.66	23.00±1.88	23.07±1.43
95	24.07±1.37	23.33±1.48	23.07±1.15

Enzymes were pre-incubated at different temperatures in the range of 40–95°C for 30 min. The remaining activity was determined with the Hide powder azure as a substrate under standard assay conditions (see Materials and Methods). Activity was expressed as a percentage of the value at 40°C, which was taken as 100%. ATCC – reference strain, PA9 and PA18 – clinical isolates. The results are presented as ±S.D. from three independent experiments. Percent of activity at corresponding incubation temperatures were statistically significant ($p < 0.05$), as determined by analysis of variance (ANOVA).

bath. As presented in Fig. 2, the proteases pre-incubated at 40°C exhibited the highest activity (Fig. 2A, Table 1). The enzymes pre-treated at 50°C and 60°C retained 86–95% and 45–60% of the activity, respectively, whereas a gradual decrease in the activity level was noticed after pre-incubation at higher temperatures (70–80°C). However, the proteases still exhibited 15% of the maximum activity after 30-min pre-incubation at 80°C (Fig. 2A). Surprisingly, after pre-treatment at 90°C and 95°C, the proteolytic activity was higher in comparison to the enzymes pre-incubated at 80°C. The activity level was only slightly lower than the one obtained for the 70°C pre-treated proteases (Fig. 2A).

In accordance with these results, only a trace signal was recognized by the anti-AP antibodies in the enzyme preparations pre-incubated at temperatures higher than 60°C and separated by native-PAGE, in contrast to the clear signal detected in the preparations pre-incubated at lower temperatures (Fig. 2B). Interestingly, the proteases pre-treated at 90°C and 95°C were better recognized by the antibodies than the 70°C and 80°C pre-incubated enzymes. However, the loss of the AP protein in preparations exposed to higher temperatures was not responsible for the observed effect, because anti-AP antibodies recognized an equally strong signal in the pre-incubated enzyme preparations separated by SDS-PAGE, regardless of the pre-treatment temperature (Fig. 3A). These results suggested different alterations in the spatial conformation of the enzyme molecules occurring depending on the temperature conditions and finally resulting in gradual loss of activity. Such alterations, by affecting accessibility of different epitopes, may also explain the observed weak binding of the anti-AP antibodies after native-PAGE (Fig. 2B).

Unexpectedly, when the activity of the proteases pre-incubated for 30 min at temperatures of 60–95°C was assayed by zymography after SDS-PAGE, the evident clear bands of gelatine proteolytic degradation were detected, even after thermal denaturation at the highest temperature used (Fig. 3B). These results suggest that the studied alkaline proteases exhibit a high renaturation capability. After being further subjected to additional denaturing conditions during SDS-PAGE, they regained the native spatial conformation and activity upon appropriate zymography conditions. In contrast, the enzymatic activity of the other extracellular metalloprotease, elastase B, produced by the three *P. aeruginosa* strains used, especially during growth in the LB medium (Andrejko *et al.*, 2013), was not restored when tested under the same conditions after thermal denaturation (Fig. 3C, D), further supporting the high renaturation capability of the studied AP proteins.

Spectroscopic analyses

To elucidate whether the intrinsic capability of renaturation could be, at least in part, responsible for the effects described above, AP produced by *P. aeruginosa* PA18 was analyzed by steady-state fluorescence spectroscopy and Fourier transform infrared spectroscopy after thermal denaturation at 60°C and 90°C.

Because fluorescence signals are very sensitive to the conformational organization of the macromolecule (Lakowicz, 1999), changes in the molecular organization of the enzyme associated with denaturation and renaturation were examined using steady-state fluorescence spectroscopy (Chanchal *et al.*, 2014; Ghisaidoobe & Chung, 2014). In order to verify the denaturation of the protease under the high temperature treatment, fluorescence spectra of native protein and protein incubated at 60°C for 30 min were measured. The spectra were detected at 23°C and 60°C, respectively. Measurement of

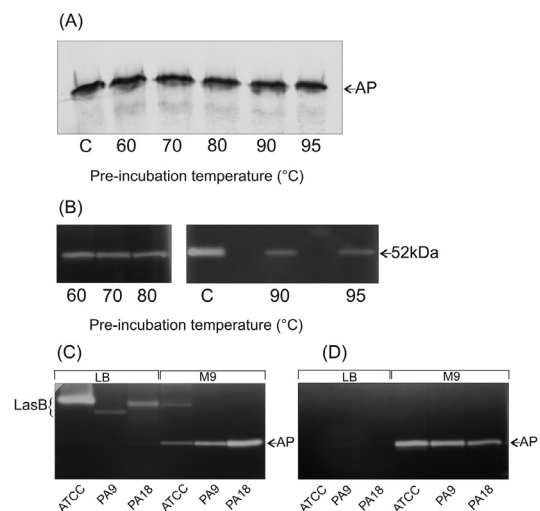


Figure 3. Immunodetection (A) and zymography analysis (B) of thermally pre-treated *P. aeruginosa* PA18 alkaline protease.

The enzyme was pre-incubated at 60–95°C for 30 min and subjected to SDS-PAGE and immunoblotting (A) or zymography (B) as described in Materials and Methods. C – control (non-temperature treated) sample. Similar results were obtained for alkaline proteases of two other *P. aeruginosa* strains studied. The renaturation ability of *P. aeruginosa* elastase B was additionally analyzed (C, D). Post-culture fluids (after 24 h of culture) of *P. aeruginosa* strains grown in the LB and M9 medium were pre-incubated at 60°C (C) and 85°C (D) for 10 min. The enzyme activities were determined by zymography after non-reducing SDS-PAGE as described in Materials and Methods. The zymograms shown are typical representatives of at least five independent experiments. The positions of alkaline protease (AP) and elastase B (LasB) are marked. ATCC – reference strain, PA9 and PA18 – clinical isolates.

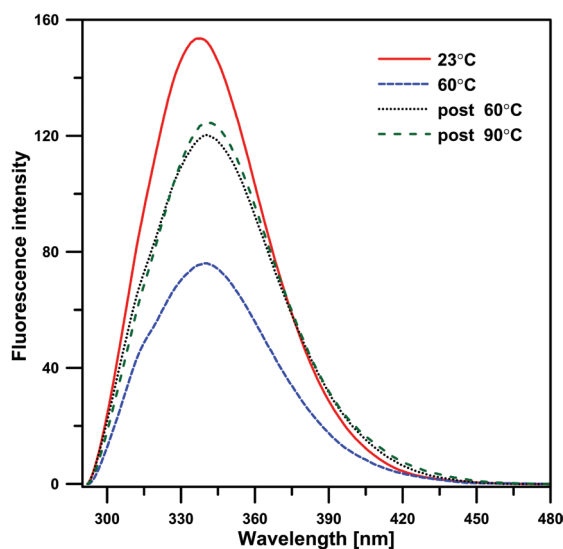


Figure 4. Fluorescence emission spectra of *P. aeruginosa* PA18 alkaline protease.

The enzyme was pre-incubated at 60°C and 90°C for 30 min and then cooled for 30 min at 4°C. Solid red line – sample before heat treatment (23°C), dashed blue line – sample heated at 60°C, dotted black line – sample heated at 60°C and cooled for 30 min at 4°C (post 60°C), dashed green line – sample heated at 90°C and cooled for 30 min at 4°C (post 90°C). Excitation at 280 nm. More details are provided in the Materials and Methods section.

the fluorescence spectrum at 90°C was impossible due to equipment limitations. As presented in Fig. 4, the maximum of the fluorescence emission spectrum of the native protein was centred at 337 nm. Since typical tryptophan fluorescence emission in a water solution at neutral pH is located at 348 nm, the blue shift of maximum fluorescence emission from the native enzyme indicated that tryptophan residues are buried in a hydrophobic environment within the protein (Lakowicz, 1999; Moller & Denicola, 2002; Ghisaidoobe & Chung, 2014). Heat treatment (60°C) decreased the intrinsic protein fluorescence intensity by approx. 50% and red-shifted the maximum fluorescence to 340 nm. In order to confirm protein renaturation, the fluorescence emission spectra of the protein samples pre-incubated at 60°C or 90°C and next cooled for 30-min at 4°C were measured (Fig. 4). Surprisingly, the value of fluorescence intensity recovered to about 80% of the fluorescence intensity of the native protein. This result indicated the recovery of the enzyme molecular conformation after protein cooling, although not completely. Figure 5A shows the fluorescence emission spectra presented in Fig. 4 normalized to get the same area beneath each spectrum. This analysis allowed determination of the relative abundance of different molecular forms of the protein in the samples with its native, denatured, or renatured form. As can be seen from the difference spectrum (Fig. 5B), the heat-induced (60°C) protein denaturation was associated with a slight bathochromic spectral shift of the main emission band and with appearance of a new spectral form which gave rise to fluorescence emission band centred at 377 nm. This band had even higher intensity in the case of the renatured samples; the highest intensity was detected for the protein pre-treated at 90°C.

The changes in the secondary structure of the protein are closely correlated with the wavenumber position and the shape of the amide I band (Goormaghtigh *et al.*, 2009; Caine *et al.*, 2012). The infrared spectroscopic analysis of the amide I band revealed that the secondary

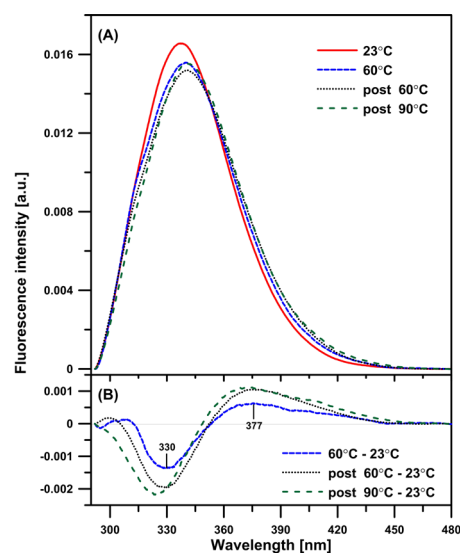


Figure 5. Normalized (A) and differential (B) fluorescence emission spectra of *P. aeruginosa* PA18 alkaline protease.

(A) The spectra were normalized to get the same area beneath each spectrum. Solid red line – sample before heat treatment (23°C), dashed blue line – sample heated at 60°C, dotted black line – sample heated at 60°C and cooled for 30 min at 4°C (post 60°C), dashed green line – sample heated at 90°C and cooled for 30 min at 4°C (post 90°C). (B) Differential spectra calculated on the basis of the spectra presented in panel (A). Excitation at 280 nm. More details are provided in the Materials and Methods section.

structure of the *P. aeruginosa* alkaline protease is mainly composed of β turns (1615 cm^{-1}) and β -pleated sheets ($1637\text{--}1623\text{ cm}^{-1}$) with a small proportion of α -helix (1655 cm^{-1}) and random coil ($1637\text{--}1645\text{ cm}^{-1}$) configurations, which is evidenced by the position of the maximum of the amide I band of *P. aeruginosa* PA 02/18 alkaline protease (Fig. 6A) and is consistent with literature data on the molecular organization of *P. aeruginosa* AP protease (Baumann *et al.*, 1993; Miyatake *et al.*, 1995; Zhang *et al.*, 2012).

The experimental procedure consisting of pre-incubation of the enzyme for 30 min at 60°C and 90°C and then cooling, exerted a slight effect on the intensity of absorbance and the shape of the amide I band (Fig. 6A–C). Pre-incubation of the alkaline protease at 60°C and 90°C decreased the intensity of amide I absorbance by 5.2% and only 4.5%, respectively. The high capability of renaturation by the analyzed enzyme is confirmed by only subtle changes in the shape of the amide I band, as shown in the differential spectra and their secondary derivatives (Fig. 6B, C). Pre-incubation at 60°C and 90°C caused a slight shift of the band, typical of the α -helix (1655 cm^{-1}), towards localization of the β -sheet band and a decrease in the β -sheet band intensity (1629 cm^{-1}), which in turn resulted in narrowing of the amide I band. Concomitantly with this decrease, a slight increase of aggregated strands ($1600\text{--}1620\text{ cm}^{-1}$) was noticed. Paradoxically, these changes exhibited higher intensity at pre-incubation of the examined enzyme at 60°C.

Sequence analysis of the *aprA* gene and AP protein in three *P. aeruginosa* strains

In order to shed light on possible determinants of the high renaturation ability, the nucleotide sequence analysis of *aprA* genes followed by analysis of their deduced amino acid sequences was carried out. The presence of *aprA* genes encoding the alkaline protease in *P. aeruginosa* PA9,

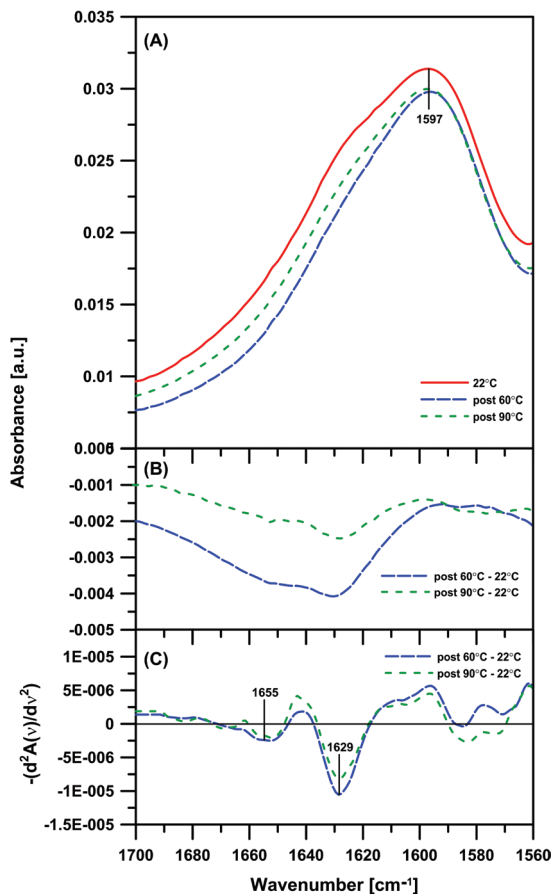


Figure 6. Fourier transform infrared spectroscopy of *P. aeruginosa* PA18 alkaline protease.

(A) FTIR spectra of the thermal processing effects on the amide I region: native protein at 22°C (solid red line), sample heated at 60°C and cooled for 30 min at 4°C (post 60° – dashed blue line), sample heated at 90°C and cooled for 30 min at 4°C (post 90°C – dashed green line). (B) Differential spectra of the amide I region obtained by subtracting the spectrum of native protein at 22°C from the spectrum of thermal processing at 60°C (post 60°C–22°C), the spectrum of native protein at 22°C subtracted from the spectrum of thermal processing at 90°C (post 90°C–22°C). (C) Second derivative spectra corresponding to (B). More details are provided in the Materials and Methods section.

PA18, and ATCC 27853 strains was confirmed in our previous report (Andrejko *et al.*, 2013). For all of the bacterial strains analysed, 1.5-kb long amplicons encompassing the whole gene for alkaline protease were obtained. The nucleotide sequence analyses of these PCR products revealed that the PA9, PA18, and ATCC 27853 strains have a functional *aprA* gene in their genomes. The genes for the alkaline protease contain a 1445-bp-long open reading frame, which begins with an ATG codon and terminates with a TGA stop codon, and encodes a 481-aa long protein. The *aprA* genes of these strains show a very high level of nucleotide sequence identity, which is 99.8% between the PA9 and PA18 strains, 99.5% between the PA 18 and ATCC 27853 strains, and 99.24% between the PA9 and ATCC 27853 strains. These genes are also highly homologous to other alkaline metalloprotease genes available in the GenBank database, having from 99% to 100% identity to the *aprA* gene of *P. aeruginosa* strain NCGM2 (accession no. AP012280), 99% identity to the *aprA* gene of *P. aeruginosa* strain PAO1 (acc. no. AE004091), and 77% identity to *Pseudomonas fluorescens* strain A506 (acc. no. AY298902). These data

indicate that genes encoding this type of enzymes are highly conserved in bacterial species. Also, at the amino acid level, the protein products of *aprA* from the *P. aeruginosa* PA9, PA18, and ATCC 27853 strains are almost identical; only three different amino acids were identified in the whole sequence of these proteins (positions 115, 209, and 437 aa) (Fig. 7). The molecular masses of these enzymes calculated from their amino acid sequences are 50.7 kDa. The AP proteins of the PA9, PA18, and ATCC 27853 strains show significant homology to enzymes belonging to alkaline metalloproteases (ZnMc-serralysin-like subfamily) containing the HEXHXUGUXH motif with three histidine residues responsible for zinc ion coordination. *P. aeruginosa* AP proteins have an identical HEIGHTLGLSH motif (conserved aa are underlined), which is located in their sequence region spanning from 187 to 197 aa. The N-terminal (1–258 aa) and C-terminal (259–481 aa) regions of these proteins comprise a Zn-binding serralysin-like domain and a peptidase M10 serralysin domain, respectively. The AP proteins of the PA9, PA18, and ATCC 27853 strains show the highest sequence homology to AP of *P. aeruginosa* PAO1 (99% identity, 100% similarity) (acc. no. NP_249940) and the alkaline metalloproteinase precursor of *P. aeruginosa* PA7 (95%/98%) (ABR83878). However, there was a high degree of homology with serralysin of *P. syringae* pv. *tabaci* ATCC 11528 (64%/76%) (EGH90818), extracellular alkaline metalloprotease AprA of *P. fluorescens* A506 (60%/73%) (AFJ54733), serralysin-like metalloprotease of *P. putida* (65%/77%) (WP_038994098), and serralysin of *Serratia marcescens* SM6 (54%/68%) (P23694). These data confirm that the *aprA* genes identified in the genomes of the *P. aeruginosa* PA9, PA18, and ATCC 27853 strains encode proteins whose sequences are very similar to each other and highly conserved in the *Pseudomonas* species. Among these three AP proteins, enzymes from PA9 and PA18 proved to be the most similar but more distantly located in relation to that from strain ATCC 27853.

DISCUSSION

In the study presented here, alkaline proteases of three *P. aeruginosa* strains were obtained from post-culture fluids after cultivation of bacteria in the synthetic minimal M9 medium. The 52 kDa protein band was recognized by specific anti-*P. aeruginosa* alkaline protease antibodies, confirming production of this protease by all of the *P. aeruginosa* strains studied. The results of sequence analyses and similarity searches provided clear evidence that each of the three proteases can be undoubtedly classified as an *P. aeruginosa* alkaline protease.

The studied proteases retained 45–60% of their activity after pre-treatment at 60°C, and 15% of the activity after 30 min pre-incubation at 80°C. Interestingly, pre-incubation at 90–95°C resulted in a higher activity level than at 80°C, suggesting that the treatment at these temperatures induced different alterations in the protein molecular organization. The retention of partial activity after heat treatment and subsequent cooling pointed toward a high renaturation capability of the *P. aeruginosa* alkaline proteases, an attribute that has not been reported earlier. In comparison to some alkaline proteases of other *P. aeruginosa* strains reported in the literature, the studied enzymes were even more thermostable. Bayouhd and others (Bayouhd *et al.*, 2000) reported that the alkaline protease of the MN1 strain retained more than 90% and 66% of the initial activity after 15 and 120 min

incubation at 60°C, respectively, but it completely lost the activity after 15 min incubation at 80°C. The alkaline protease of *P. aeruginosa* strain K was completely inactivated upon incubation at 80°C for 30 min (Rahman *et al.*, 2006).

Steady-state fluorescence spectroscopy was used to examine changes in the molecular organization of the alkaline protease of *P. aeruginosa* PA18 associated with its heat-induced denaturation and renaturation. As expected, the high temperature affected the enzyme's spatial structure. However, after cooling, the value of fluorescence intensity of the 60°C- and 90°C-pre-treated enzyme was only 20% lower than the value of fluorescence intensity of the native protein, indicating the high level of recovery of the enzyme's spatial conformation. The fluorescence changes detected at 60°C (a shift of the maximum fluorescence from 337 nm to 340 nm) may indicate an increase in the exposure of tryptophan residues to the polar solvent resulting from the thermal protein unfolding (Lakowicz, 1999; Uttam *et al.*, 2011; Zhang *et al.*, 2012; Ghisaidoobe & Chung, 2014). On the other hand, it cannot be excluded that the observed decrease in fluorescence intensity at this temperature may also result from the effect of temperature on the fluorescence emission intensity. It is known that fluorescence intensity of aromatic amino acids decreases along with an increase in the temperature of the sample (Gally & Edelman, 1962). The appearance of the band at a longer wavelength, mainly after cooling (377 nm), can be attributed to protein fluorophore aggregates resulting from the formation of a large macromolecular protein structure (Lakowicz, 1999). It was demonstrated that the RTX-containing domain of *P. aeruginosa* alkaline protease can form polymers (Zhang *et al.*, 2014), a feature that may be involved in the observed changes. The higher level of oligomerization after the 90°C pre-treatment in comparison to the pre-treatment at 60°C, may also contribute to the lower level of activity of the renatured enzyme pre-incubated at 90°C. In addition, molecular oligomers are known as very effective fluorescence quenchers (Bhattacharya *et al.*, 2011; Hong *et al.*, 2011). Hence, the partial protein oligomerization, in addition to the possible protein unfolding, can explain the lack of total recovery of the alkaline protease fluorescence intensity. A similar effect was reported for recombinant *Acinetobacter baylyi* diketoreductase. An analysis of thermal-induced unfolding and renaturation of this enzyme indicated that renaturation from 90°C and 80°C was more complete than that from 70°C and 60°C, with a tendency of better recovery of enzymatic activity from higher unfolding temperatures. The phenomenon was explained by a collective contribution of partial aggregation and structural changes occurring in the protein molecules (Lu *et al.*, 2010). In turn, results of a study performed on *Escherichia coli* γ -glutamyltranspeptidase, a hetero-dimeric enzyme, suggested that structural features of a large subunit were important for the renaturation process after thermal denaturation (Van Ho *et al.*, 2013). Interestingly, presence of an additional loop composed of 12 residues in the C-terminal segment of the *Bacillus subtilis* γ -glutamyltranspeptidase large subunit caused steric perturbations and prevented reconstitution of the active hetero-dimer complex after thermal denaturation (Van Ho *et al.*, 2013).

Analysis of the secondary structure based on infrared absorption spectroscopy (FTIR) confirmed the high renaturation capability of the studied alkaline protease. The results did not show any clear changes in the α -helix

configuration (1655 cm^{-1}) and extension of the β -sheet band within amide I. This suggested recovery of the secondary structure of the enzyme subjected to pre-incubation at 60°C and 90°C. However, the slight decrease in β -sheet band intensity concomitantly with the increase at 1600–1620 cm^{-1} could suggest partial protein aggregation (Tamm & Tatulian, 1997). It was demonstrated that a function of temperature is a decrease in predominantly secondary structural element, β -sheet or α -helix, which is replaced by intermolecular β -sheet structure common in the aggregated state of proteins (Dong *et al.*, 1997; Dong *et al.*, 2000; Kong & Yu, 2007).

The results indicated an intrinsic ability of the studied alkaline proteases to partially regain spatial conformation after thermal denaturation and subsequent cooling, which allowed partial recovery of activity. After exposure to further denaturing conditions (SDS), the enzymes were even more prone to renaturation, which was clearly evidenced by zymography. Most probably, an important factor in this process was the presence of calcium ions in a zymography buffer, known to induce proper folding and stabilization of a *P. aeruginosa* alkaline protease (Zhang *et al.*, 2012).

The high identity of the nucleotide and amino acid sequence of the studied alkaline proteases with alkaline metalloproteases produced by other *P. aeruginosa* strains suggests that the renaturation capability reported here may be a common feature of *P. aeruginosa* alkaline proteases. As mentioned, Zhang and others (Zhang *et al.*, 2012; Zhang *et al.*, 2014) reported on the role of calcium ions in induction of proper folding and stabilization of the molecular spatial conformation of a *P. aeruginosa* alkaline protease. In single site mutation experiments in which a Val residue located centrally in the interface between the RTX and proteinase domains was replaced by an Asp residue (V280D), they demonstrated that disruption of the domain-domain interface had reduced the protease activity and that proper association between these two domains is important for folding and activity of AP. Furthermore, truncation or disruption (A5D, V9D, F12D) of the N-terminal α -helix caused a decrease in the AP stability, suggesting a critical role for interactions between this α -helix and RTX domain for native state stability (Zhang *et al.*, 2012). The alkaline protease, as other RTX-containing proteins, is secreted by the Type 1 secretion system (T1SS). Due to the physical constrains of this system, most probably the protein has to be unfolded during the secretion process and becomes folded at an appropriate concentration of calcium ions once secreted outside the cell. The high renaturation capability of *P. aeruginosa* alkaline protease demonstrated in this paper may additionally facilitate effective folding of the molecule after secretion, thereby contributing to the enzymatic activity. Exploring AP properties that influence its folding provides further insight into understanding the mechanisms of virulence of *Pseudomonas* and other Gram-negative bacteria that utilize RTX-containing virulence factors. Actually, production of this type of proteins may favour bacteria in the competition with other microorganisms fighting for the same niche inside the body of an infected host, as well as in the external environment.

Acknowledgements

The authors acknowledge the technical assistance of Monika Koziej. We thank Prof. E.A. Trafny (Department of Microbiology and Epidemiology, Military Institute of Hygiene and Epidemiology in Warsaw, Poland)

for providing the clinical isolates of *P. aeruginosa*. We are grateful to Dr. R. Voulhoux (Laboratoire d'Ingénierie des Systèmes Macromoléculaires, CNRS UMR7255, Institut de Microbiologie de la Méditerranée, France) for the anti-alkaline protease antibodies.

REFERENCES

- Andrejko M, Mizerska-Dudka M (2012) Effect of *Pseudomonas aeruginosa* elastase B on level and activity of immune proteins/peptides of *Galleria mellonella* hemolymph. *J Insect Sci* **12**: 88. <https://doi.org/10.1673/031.012.8801>
- Andrejko M, Zdybicka-Barabas A, Janczarek M, Cytirńska M (2013) Three *Pseudomonas aeruginosa* strains with different protease profiles. *Acta Biochim Pol* **60**: 83–90
- Baumann U, Wu S, Flaherty KM, McKay DB (1993) Three-dimensional structure of the alkaline protease of *Pseudomonas aeruginosa*: a two-domain protein with a calcium binding parallel beta roll motif. *EMBO J* **12**: 3357–3364. PMID: PMC413609
- Bayoudh A, Gharsallah N, Chamkha M, Dhouib A, Ammar S, Nasri M (2000) Purification and characterization of an alkaline protease from *Pseudomonas aeruginosa* MN1. *J Ind Microbiol Biotechnol* **24**: 291–295. <https://doi.org/10.1038/sj.jim.2900822>
- Bhattacharya M, Jain M, Mukhopadhyay S (2011) Insights into the mechanism of aggregation and fibril formation from bovine serum albumin. *J Phys Chem B* **115**: 4195–4205. <https://doi.org/10.1021/jp111528c>
- Blake MS, Johnston KH, Russell-Jones GJ, Gotschlich EC (1984) A rapid, sensitive method for detection of alkaline phosphatase-conjugated anti-antibody on Western blots. *Anal Biochem* **136**: 175–179. [https://doi.org/10.1016/0003-2697\(84\)90320-8](https://doi.org/10.1016/0003-2697(84)90320-8)
- Bradford MM (1976) A rapid and sensitive method for quantitation of microgram quantities of protein utilizing the principle of protein-dye binding. *Anal Biochem* **72**: 248. [https://doi.org/10.1016/0003-2697\(76\)90527-3](https://doi.org/10.1016/0003-2697(76)90527-3)
- Butterworth MB, Zhang L, Heidrich EM, Myerburg MM, Thibodeau PH (2012) Activation of the epithelial sodium channel (ENaC) by the alkaline protease from *Pseudomonas aeruginosa*. *J Biol Chem* **287**: 32556–32565. <https://doi.org/10.1074/jbc.M112.369520>
- Caballero AR, Moreau JM, Engel LS, Marquart ME, Hill JM, O'Callaghan RJ (2001) *Pseudomonas aeruginosa* protease IV enzyme assays and comparison to other *Pseudomonas* proteases. *Anal Biochem* **290**: 330–337. <https://doi.org/10.1006/abio.2001.4999>
- Caine S, Heraud P, Tobin MJ, McNaughton D, Bernard CC (2012) The application of Fourier transform infrared microspectroscopy for the study of diseased central nervous system tissue. *Neuroimage* **59**: 3624–3640. <https://doi.org/10.1016/j.neuroimage.2011.11.033>
- Chanchal H, Tuhin S, Venkataramanan M (2014) A resonance energy transfer approach for the selective detection of aromatic amino acids. *J Mater Chem C* **47**: 10157–10163. <https://doi.org/10.1039/C4TC01954G>
- Dong A, Kendrick B, Kreilgard L, Matsuura J, Manning MC, Carpenter JF (1997) Spectroscopic study of secondary structure and thermal denaturation of recombinant human factor XIII in aqueous solution. *Arch Biochem Biophys* **347**: 213–220. <https://doi.org/10.1006/abbi.1997.0349>
- Dong A, Randolph TW, Carpenter JF (2000) Entrapping intermediates of thermal aggregation in α -helical proteins with low concentration of guanidine hydrochloride. *J Biol Chem* **275**: 27689–27693. <https://doi.org/10.1074/jbc.M005374200>
- Duong F, Lazdunski A, Cami B, Murgier M (1992) Sequence of a cluster of genes controlling synthesis and secretion of alkaline proteinase in *Pseudomonas aeruginosa*: relationships to other secretory pathways. *Gene* **121**: 47–54. [https://doi.org/10.1016/0378-1119\(92\)90160-Q](https://doi.org/10.1016/0378-1119(92)90160-Q)
- Duong F, Lazdunski A, Murgier M (1996) Protein secretion by heterologous bacterial ABC-transporters: the C-terminus secretion signal of the secreted protein confers high recognition specificity. *Mol Microbiol* **21**: 459–470. <https://doi.org/10.1111/j.1365-2958.1996.tb02555.x>
- Feltzer RE, Gray RD, Dean WL, Pierce WM Jr (2000) Alkaline proteinase inhibitor of *Pseudomonas aeruginosa*. Interaction of native and N-terminally truncated inhibitor proteins with *Pseudomonas* metalloproteinases. *J Biol Chem* **275**: 21002–21009. <https://doi.org/10.1074/jbc.M00208820>
- Gally JA, Edelman GM (1962) The effect of temperature on the fluorescence of some aromatic amino acids and proteins. *Biochem Biophys Acta* **60**: 499–509. [https://doi.org/10.1016/0006-3002\(62\)90869-7](https://doi.org/10.1016/0006-3002(62)90869-7)
- Ghisaidoobe ABT, Chung SJ (2014) Intrinsic tryptophan fluorescence in the detection and analysis of proteins: a focus on Förster resonance energy transfer techniques. *Int J Mol Sci* **15**: 22518–22538. <https://doi.org/10.3390/ijms15122518>
- Goormaghtigh E, Gasper R, Bénard A, Goldsztein A, Raussens V (2009) Protein secondary structure content in solution, films and tissues: Redundancy and complementarity of the information content in circular dichroism, transmission and ATR FTIR spectra. *Biochim Biophys Acta* **1794**: 1332–1343. <https://doi.org/10.1016/j.bbapap.2009.06.007>
- Guyot N, Bergsson G, Butler MW, Greene CM, Weldon S, Kessler E, Levine RI, O'Neill SJ, Taggart CC, McElvaney NG (2010) Functional study of elafin cleaved by *Pseudomonas aeruginosa* metalloproteinases. *Biol Chem* **391**: 705–716. <https://doi.org/10.1515/BC.2010.066>
- Guzzo J, Pages J-M, Duong F, Lazdunski A, Murgier M (1991) *Pseudomonas aeruginosa* alkaline protease: evidence for secretion genes and study of secretion mechanism. *J Bacteriol* **173**: 5290–5297. PMID: PMC208238
- Hoge R, Pelzer A, Rosenau F, Wilhelm S (2010) Weapons of a pathogen: proteases and their role in virulence of *Pseudomonas aeruginosa*. In *Current Research, Technology and Education Topics in Applied Microbiology and Microbial Biotechnology*, number 2. Mendez-Vilas A, ed, pp 383–395. Microbiology book series, Formatex Research Center.
- Hong YQ, Ghebrehiwet B (1992) Effect of *Pseudomonas aeruginosa* elastase and alkaline protease on serum complement and isolated components C1q and C3. *Clin Immunol Immunopathol* **62**: 133–138. PMID: 1730152
- Hong Y, Lamab YWI, Tang BZ (2011) Aggregation-induced emission. *Chem Soc Rev* **40**: 5361–5388. <https://doi.org/10.1039/c1cs15113d>
- Horvat RT, Parmely MJ (1988) *Pseudomonas aeruginosa* alkaline protease degrades human gamma interferon and inhibits its bioactivity. *Infect Immun* **56**: 2925–2932. PMID: PMC259672
- Howe TR, Iglewski BH (1984) Isolation and characterization of alkaline protease-deficient mutants of *Pseudomonas aeruginosa* in vitro and in a mouse eye model. *Infect Immun* **43**: 1058–1063. PMID: PMC264293
- Kong J, Yu S (2007) Fourier transform infrared spectroscopic analysis of protein secondary structures. *Acta Biochim Biophys Sin* **39**: 549–559. <https://doi.org/10.1111/j.1745-7270.2007.00320.x>
- Laemmli UK (1970) Cleavage of structural proteins during the assembly of the head of bacteriophage T4. *Nature* **227**: 680–685. <https://doi.org/10.1038/227680a0>
- Lakowicz JR (1999) in *Principles of fluorescence spectroscopy*, Kluwer Academic Publishers, New York. <https://doi.org/10.1007/978-1-4757-3061-6>
- Leidal KG, Munson KL, Johnson MC, Denning GM (2003) Metalloproteases from *Pseudomonas aeruginosa* degrade human RANTES, MCP-1, and ENA-78. *J Interf Cytok Res* **23**: 307–318. <https://doi.org/10.1089/107999003766628151>
- Lu M, Cao X, Yang X, Zheng H, Liu N, Jiang Y, Lin D, Chen Y (2010) A diketoreductase exhibits unique renaturation profile from thermal-induced protein unfolding. *Amino Acids* **39**: 609–613. <https://doi.org/10.1007/s00726-010-0491-9>
- Miyatake H, Hata Y, Fujii T, Hamada K, Morihara K, Katsube Y (1995) Crystal structure of the unliganded alkaline protease from *Pseudomonas aeruginosa* IF03O8O and its conformational changes on ligand binding. *J Biochem* **118**: 474–479. PMID: 8690704
- Moller M, Denicola A (2002) Protein tryptophan accessibility studied by fluorescence quenching. *Bioch Mol Biol Edu* **30**: 175–178. <https://doi.org/10.1002/bmb.2002.494030030035>
- Okuda K, Morihara K, Atsumi Y, Takeuchi H, Kawamoto S, Kawasaki H, Suzuki K, Fukushima J (1990) Complete nucleotide sequence of the structural gene for alkaline proteinase from *Pseudomonas aeruginosa* IF03455. *Infect Immun* **58**: 4083–4088. PMID: PMC313780
- Parmely M, Gale A, Clabaugh M, Horvat R, Zhou WW (1990) Proteolytic inactivation of cytokines by *Pseudomonas aeruginosa*. *Infect Immun* **58**: 3009–3014. PMID: PMC313603
- Patil U, Chaudhari A (2009) Purification and characterization of solvent-tolerant, thermostable, alkaline metalloprotease from alkalophilic *Pseudomonas aeruginosa* MTCC 7926. *J Chem Technol Biotechnol* **284**: 1255–1262
- Rahman RNZ, Geok LP, Basri M, Salleh AB (2006) An organic solvent-stable alkaline protease from *Pseudomonas aeruginosa* strain K: enzyme purification and characterization. *Enzyme Microb Tech* **39**: 1484–1491
- Rawlings ND, Barrett AJ, Bateman A (2010) MEROPS: the peptidase database. *Nucl Acids Res* **38**: 227–233. <https://doi.org/10.1093/nar/gkp971>
- Sambrook J, Fritsch EF, Maniatis T (1989) in *Molecular Cloning: A Laboratory Manual*, Cold Spring Harbor Laboratory Press, New York.
- Sievers F, Wilm A, Dineen D, Gibson TJ, Karplus K, Li W, Lopez R, McWilliam H, Remmert M, Soding J, Thompson JD, Higgins DG (2011) Fast, scalable generation of high-quality protein multiple sequence alignments using Clustal Omega. *Mol Syst Biol* **7**: 539. <https://doi.org/10.1038/msb.2011.75>
- Tamm LK, Tatulian SA (1997) Infrared spectroscopy of proteins and peptides in lipid bilayers. *Q Rev Biophys* **30**: 365–429. PMID: 9634652
- Twining SS, Kirschner SE, Mahnke LA, Frank DW (1993) Effects of *Pseudomonas aeruginosa* elastase, alkaline protease and exotoxin A on corneal proteases and proteins. *Invest Ophthalmol Visual Sci* **34**: 2699–2712. PMID: 8344792

- Uttam A, Chandrima J, Saptarshi M (2011) Protein unfolding and subsequent refolding: a spectroscopic investigation. *Phys Chem Chem Phys* **13**: 20418–20426. <https://doi.org/10.1039/c1cp21759c>
- Van Ho T, Kamei K, Wada K, Fukuyama K, Suzuki H (2013) Thermal denaturation and renaturation of γ -glutamyltranspeptidase of *Escherichia coli*. *Biosci Biotechnol Biochem* **77**: 409–412. <https://doi.org/10.1271/bbb.120780>
- Zhang L, Conway JF, Thibodeau PH (2012) Calcium-induced folding and stabilization of the *Pseudomonas aeruginosa* alkaline protease. *J Biol Chem* **287**: 4311–22. <https://doi.org/10.1074/jbc.M111.310300>
- Zhang L, Franks J, Stolz DB, Conway JF, Thibodeau PH (2014) Inducible polymerization and two-dimensional assembly of the repeats-in-toxin (RTX) domain from the *Pseudomonas aeruginosa* alkaline protease. *Biochemistry* **53**: 6452–6462. <https://doi.org/10.1021/bi5007546>